



THE UNIVERSITY *of* EDINBURGH

Edinburgh Research Explorer

Solid-Liquid Equilibria for the CO₂+R23 and N₂O+R23 Systems

Citation for published version:

Di Nicola, G, Giuliani, G, Polonara, F, Santori, G & Stryjek, R 2010, 'Solid-Liquid Equilibria for the CO₂+R23 and N₂O+R23 Systems' International journal of thermophysics, vol 31, no. 10, pp. 1880-1887., 10.1007/s10765-008-0511-0

Digital Object Identifier (DOI):

[10.1007/s10765-008-0511-0](https://doi.org/10.1007/s10765-008-0511-0)

Link:

[Link to publication record in Edinburgh Research Explorer](#)

Document Version:

Author final version (often known as postprint)

Published In:

International journal of thermophysics

Publisher Rights Statement:

The final publication is available at Springer via <http://dx.doi.org/10.1007/s10765-008-0511-0>

General rights

Copyright for the publications made accessible via the Edinburgh Research Explorer is retained by the author(s) and / or other copyright owners and it is a condition of accessing these publications that users recognise and abide by the legal requirements associated with these rights.

Take down policy

The University of Edinburgh has made every reasonable effort to ensure that Edinburgh Research Explorer content complies with UK legislation. If you believe that the public display of this file breaches copyright please contact openaccess@ed.ac.uk providing details, and we will remove access to the work immediately and investigate your claim.



SOLID-LIQUID EQUILIBRIA FOR THE CO₂ + R23, AND N₂O + R23 SYSTEMS

Giovanni Di Nicola,* Giuliano Giuliani, Fabio Polonara, Giulio Santori, and Roman Stryjek

¹Dipartimento di Energetica, Università Politecnica delle Marche, Via Brecce Bianche 60100,
Ancona, Italy.

²Institute of Physical Chemistry, Polish Academy of Sciences, Warsaw, Poland.

* Author to whom correspondence should be addressed.

E-mail: g.dinicola@univpm.it

Paper presented at the 8th Asian Thermophysical Properties Conference 21-24 August, 2007, Fukuoka, Japan

Abstract

A recently built experimental set-up was employed for the estimation of the solid-liquid equilibria of alternative refrigerant systems. In this paper two binaries, i.e., carbon dioxide + trifluoromethane ($\text{CO}_2 + \text{R23}$) and nitrous oxide + trifluoromethane ($\text{N}_2\text{O} + \text{R23}$), were studied down to temperatures of 117 K. In order to check the reliability of the apparatus, the triple points of the pure fluids contained in the mixture were measured, revealing good consistency with the literature.

The results obtained for the mixtures were interpreted by means of the Schröder equation.

Keywords: Cascade units, Eutectic, Refrigerants, Solid-liquid equilibria.

1 Introduction

In the design of cryogenic processes, it is frequently necessary to estimate the solid-liquid equilibria (SLE) and the eutectic composition of a mixture. The data on SLE are important in the refrigeration industry, defining the lowest temperature limit at which the refrigerant may circulate in the fluid state. In addition, SLE provide theoretical information on the behavior of studied systems at low temperatures in terms of activity coefficients. In spite of this, the SLE for HFC refrigerants are extremely scarce in the literature.

Due to the expected temperatures of the SLE of systems formed with CO₂ and/or N₂O + HFC refrigerants that usually span from about 100 K up to 217 K (in case of CO₂ as the mixture component), SLE measurements generally creates difficulties in the visual observation of the disappearance of the last amount of the solid phase. Hence, a set-up was specifically built [1] avoiding the need of visual observation of phase behavior. Recently, this set-up was used to study the SLE of the CO₂ + R125 and N₂O + R125 systems [1], CO₂ + N₂O, CO₂ + R32, and N₂O + R32 systems [2], and CO₂ + R152a and N₂O + R152a systems [3]. In this paper, the system's behavior was measured down to temperatures of 117 K for two binaries, i.e., CO₂ + R23 and N₂O + R23.

2 Description of the apparatus

2.1 Measurement cell. The experimental set-up is shown in Fig. 1. It is the same as already described elsewhere [1-3], so it will be only briefly described here. The measuring cell (1), with a volume of approximately 47 cm³, was made out of a stainless-steel cylinder. A stirrer (3) was placed in the cell. The stirrer inside the cell was turned by a magnet (4). Two holes were made in the cover and a stainless-steel tube was inserted through and welded to the first hole for charging the cell with gas, while the second hole was used to contain the platinum resistance thermometer (Pt 100 Ω, Minco, Mod. S7929) (2). The magnet was housed in a seat made of brass, which was

connected to the shaft of an electric engine (5) driving the rotation of the magnet and thus also of the stirrer inside the cell.

The cooling system included four parts:

1. A coil consisting of a copper tube, placed inside a Dewar filled with liquid nitrogen (6), which absorbs heat from the carrier fluid (compressed air) flowing inside it;
2. A coil with the same structural features as above, wrapped around the measuring cell and removing heat from the cell by surface contact due to the cold air circulating inside it. The assembly consisting of the coil and the cell was placed inside a second Dewar (7) so as to increase its thermal isolation;
3. A double pipe heat exchanger (8) for the carrier fluid pre-cooling. A flow of air at room temperature entered the exchanger's inner tube and, as it moved through the tube, it was cooled by the backflow heat exchange with the cold air leaving the coil wrapped around the measuring cell;
4. An ice trap (9) to ensure the stratification on the inside walls of the ice that forms after the liquefaction and subsequent solidification of the humidity in the carrier fluid circulating in the first coil.

A dry air supplier (10) was installed to overcome any problems related to air humidity. A mass flow control was installed upstream from the dehumidifier (11). The airflow was also measured by a rotameter (12). An absolute pressure transducer (HBM, Mod. P8A) (13) was also installed in the charging tube.

3 Experimental procedure and uncertainties

3.1 Experimental procedure. The bottle containing the refrigerant gas (14) was weighed on the electronic balance; then the bottle was connected to the apparatus and to the vacuum pump (15) (Vacuubrand, Mod. RZ2). A vacuum was created inside the measuring cell and the charging tube as recorded on the vacuum pump gauge (Galileo, Mod. OG510). Then the fluid was charged by

opening the valve on the gas bottle. The temperature of the cell was decreased by a flow of compressed air cooled with liquid nitrogen so as to insert the whole mass in the cell, leaving as little as possible in the charging tube. Then the on/off valve was closed; and the gas bottle was disconnected and weighed again to establish the actual mass charged in the cell.

The air was cooled by putting the coil inside a Dewar filled with liquid nitrogen. The coil was then wrapped around the measuring cell. During the measurement procedure, the temperature of the sample inside the cell was carefully controlled to fall at a uniform rate by the air flowing inside the coil. Monitoring the time dependence of the temperature, a cooling curve was obtained for each sample concentration. While the change of phase occurs, the heat removed by cooling is compensated by the latent heat of the phase change, resulting in a temperature drop as shown in Fig. 2. The arrest in cooling during solidification allows the melting point of the material to be identified on the time-temperature curve. To give a phase diagram, the melting points can be plotted versus the composition.

The SLE data are measured with the presence of the vapor phase; however, the measured pressures are not reported here as the data were not validated as corresponding to VSLE.

3.2 Uncertainties. All the uncertainties were calculated using the law of error propagation, as reported elsewhere [1]. Here, the previously reported results will be briefly summarized.

The uncertainty in the mass of fluid charged in the measuring cell was less than 0.008 g for a pure fluid. The total uncertainty of the mass of sample mixture was less than 0.01 g. The uncertainty in composition measurements was estimated to be always less than 0.005 in mole fraction. The total uncertainty for the thermoresistance, using the law of error propagation, was calculated to be less than 0.023 K.

4 Experimental Results

4.1 Chemicals. Carbon dioxide and nitrous oxide were supplied by Sol SpA. Their purities were checked by gas chromatography, using a thermal conductivity detector, and were found to be

99.99% in mass for both fluids, basing all estimations on an area response. R23 was also supplied by Sol SpA; its purity was found to be 99.6% in mass on an area response curve.

4.2 Pure Fluids. Figure 2 shows an example of a measurement taken for carbon dioxide in which there was evidence of approximately 10 K of supercooling. Different tests were also conducted for N₂O and R23, using different configurations (with the stirrer on or off). The results for CO₂ and N₂O were reported elsewhere [2]. For R23, three measurements were carried out, giving the following results: triple point at temperatures of 117.5 K, 117.8 K, and 118.0 K. The comparison with the literature value (118.02 K [4]) shows generally good agreement in the triple-point measurements for R23. The triple-point pressure for R23 was too low to accurately measure it with the current apparatus.

4.3 Results for Mixtures. Regarding the mixtures, there are no data on SLE in the literature, so the data we obtained can be used as the starting point for future studies. Measurements were taken using different concentrations of the two components, obtaining a satisfactory number of points, which were then recorded on a concentration/temperature (T - x) graph.

Since the measured vapor-pressure data were not accurately measured at very low temperatures within the declared precision of the used instrument (the pressure values were acquired by an absolute pressure transducer HBM, Mod. P8A, and the global uncertainty of the pressure measurements was estimated to be less than ± 3 kPa [1]), the vapor-pressure data are not reported in the present paper.

The T - x measurements for the two mixtures considered (CO₂ + R23 and N₂O + R23, respectively) are given in the Figs. 3 and 4. The results are also summarized in Table 1. From the T - x data it is evident that N₂O + R23 forms a eutectic ($x_1 = 0.08$ at $T = 115$ K). Per analogy to other studied CO₂ + HFC systems [1-3], it is expected that the CO₂ + R23 forms a eutectic as well in the very dilute region. However, due to the very dilute composition range, this assumption could not be validated experimentally.

4.4 Rossini Method Corrections. Temperature data acquisitions were corrected with the Rossini method [5] because a constant cooling rate was not guaranteed by our experimental method. This graphic method, illustrated in Fig. 2, considers the area contained by the tangent to the curve in the descending stretch after the temperature drop, and curve itself; then a vertical segment (a) is taken, which divides the area into two equal parts; then a second, horizontal segment (b) is obtained, from the point of intersection between the segment (a) and the tangent to the curve, up until it identifies the temperature corresponding to this new point on the axis of the ordinate (T_m). The entity of the corrections takes into account the fact that the fluid is still in a liquid state during the metastable state (supercooling) that precedes proper solidification. In this phase, the temperature is distinctly lower than the one characterizing the instant when crystallization begins, its amplitude depending mainly on the rate at which the temperature is lowered. The resulting corrections were nonetheless always very limited, of the order of a few tenths of a kelvin in the majority of cases, and always much less than 1 K.

5 Interpretation of the Results

The SLE depend both on the crystals formed in solution and on the properties of the liquid phase. The course of the *liquidus* is well described by the Schröder equation, known since the end of the 19th century [6]. The exact course of the *liquidus* for ideal mixtures (i.e., showing a small deviation from Raoult's law) depends mainly on the property of the solute and, in the case of non-ideal systems, on the property of the liquid phase.

The solubility of the solid solute in the solvent (here, R23) can be described by the Schröder equation; which disregarding any difference between the heat capacity of the subcooled liquid solute and solid solute takes the following form:

$$\ln \gamma_2 x_2 = -\frac{\Delta h_m}{RT} \left(1 - \frac{T}{T_m} \right) \quad (1)$$

where the subscript 2 denotes the solute and the subscript m denotes the property at the melting point. Assuming as a first approximation that the solute's activity coefficient, $\gamma_2 = 1$, we can write

$$\ln x_2 = -\frac{\Delta h_m}{RT} \left(1 - \frac{T}{T_m} \right) \quad (2)$$

This simplification leads to the consideration that the solubility of the solid solute is independent of the solvent as far as the assumptions hold. The enthalpies at the melting point (Δh_m) were assumed to be 9020 J·mol⁻¹ [7], 6540 J·mol⁻¹ [7], and 4120 J·mol⁻¹ [4], for CO₂, N₂O, and R23, respectively.

The curve of the liquidus calculated with the Schröder equation is included in Figs. 3 and 4. Both systems followed well the Schröder equation. For the CO₂ + R23 system good agreement with the equation prediction was evident. For the N₂O + R23, a general agreement with the Schröder equation was evident even if, excluding a couple of points, a systematic deviation (1 to 2) K was evident at higher N₂O concentrations.

6 Conclusion

The SLE behavior of CO₂ + R23 and N₂O + R23 was measured at temperatures down to 117 K by an apparatus that enabled us to record temperature and composition data. The triple points of the pure fluids contained in the mixture were measured, resulting in good consistency with the literature. The CO₂ + R23 system showed presumably a eutectic in the very dilute CO₂ region. The N₂O + R23 system showed a eutectic ($x_1 = 0.08$ at $T = 115$ K). The measured systems showed good agreement in terms of Schröder equation predictions.

References

1. G. Di Nicola, G. Giuliani, F. Polonara, R. Stryjek, *J. Chem. Eng. Data* **51**:2209 (2006).
2. G. Di Nicola, G. Giuliani, F. Polonara, R. Stryjek, *Fluid Phase Equilib.* **256**:86 (2007).
3. G. Di Nicola, F. Polonara, G. Santori, R. Stryjek, *J. Chem. Eng. Data* **53**:1980 (2008).

4. J. W. Magee, *Int. J. Thermophys.* **21**:1351 (2000).
5. B. J. Mair, J. A. R. Glasgow, F. D. Rossini, *J. Res. Nat. Bur. Standards* **26**:591 (1941).
6. I. Schröder, *Z. Phys. Chem.* **11**:449 (1893).
7. D. R. Lide, H. V. Kehiaian, *CRC Handbook of Thermophysical and Thermochemical Data*. CRC Press, Inc. (1994).

Figure captions

Figure 1. Schematic illustration of the apparatus.

1. Measurement cell
2. Platinum resistance thermometer
3. Stirrer
4. Magnet
5. Electric engine
6. Dewar with liquid nitrogen
7. Dewar containing the measurement cell
8. Double-pipe heat exchanger
9. Ice trap
10. Dry air supplier
11. Mass flow controller
12. Rotameter
13. Pressure trasducer
14. Charging bottle
15. Vacuum pump system

Figure 2. Acquisition of CO₂ triple-point temperature measurements and Rossini method illustration.

Figure 3. SLE for the CO₂ + R23 system. Black symbols denote the experimental points while the lines represent the Schröder eq.

Figure 4. SLE for the N₂O + R23 system. Black symbols denote the experimental points while the lines represent the Schröder eq.

Table 1 T - x Measurements for the CO₂ + R23 and N₂O + R23 Binary Systems.

CO ₂ (1) + R23 (2)		N ₂ O(1) + R23 (2)	
x_1	T (K)	x_1	T (K)
0.000	118.02	0.000	118.02
0.026	126.89	0.035	117.73
0.044	133.85	0.058	115.88
0.093	147.26	0.114	120.39
0.126	152.05	0.136	123.97
0.175	159.83	0.215	133.00
0.268	172.06	0.290	142.68
0.306	175.92	0.340	144.65
0.321	174.98	0.459	152.99
0.359	179.69	0.473	152.71
0.401	182.78	0.499	155.15
0.480	189.32	0.621	162.21
0.619	199.30	0.688	168.41
0.623	199.23	0.733	168.32
0.745	203.86	0.787	171.00
0.761	205.34	0.839	175.18
0.853	209.59	0.883	176.21
0.904	211.19	1.000	181.99
1.000	216.52		

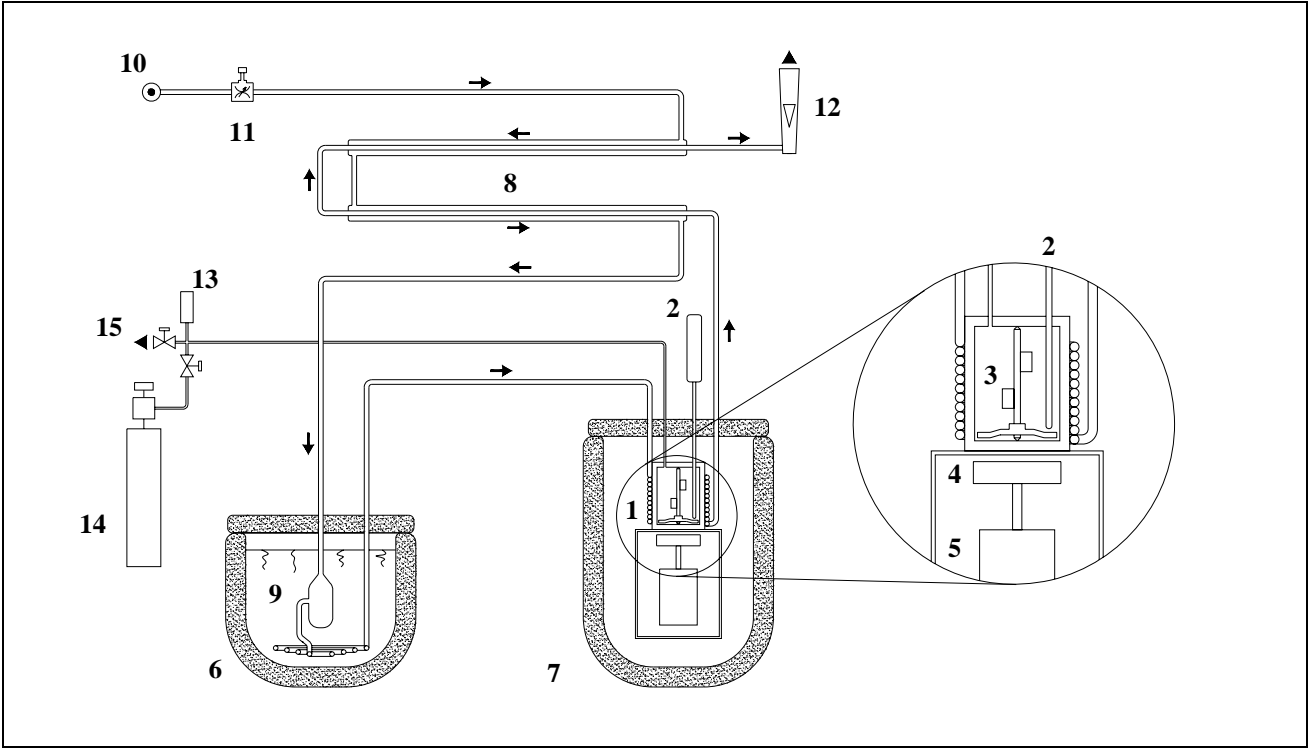


Figure 1

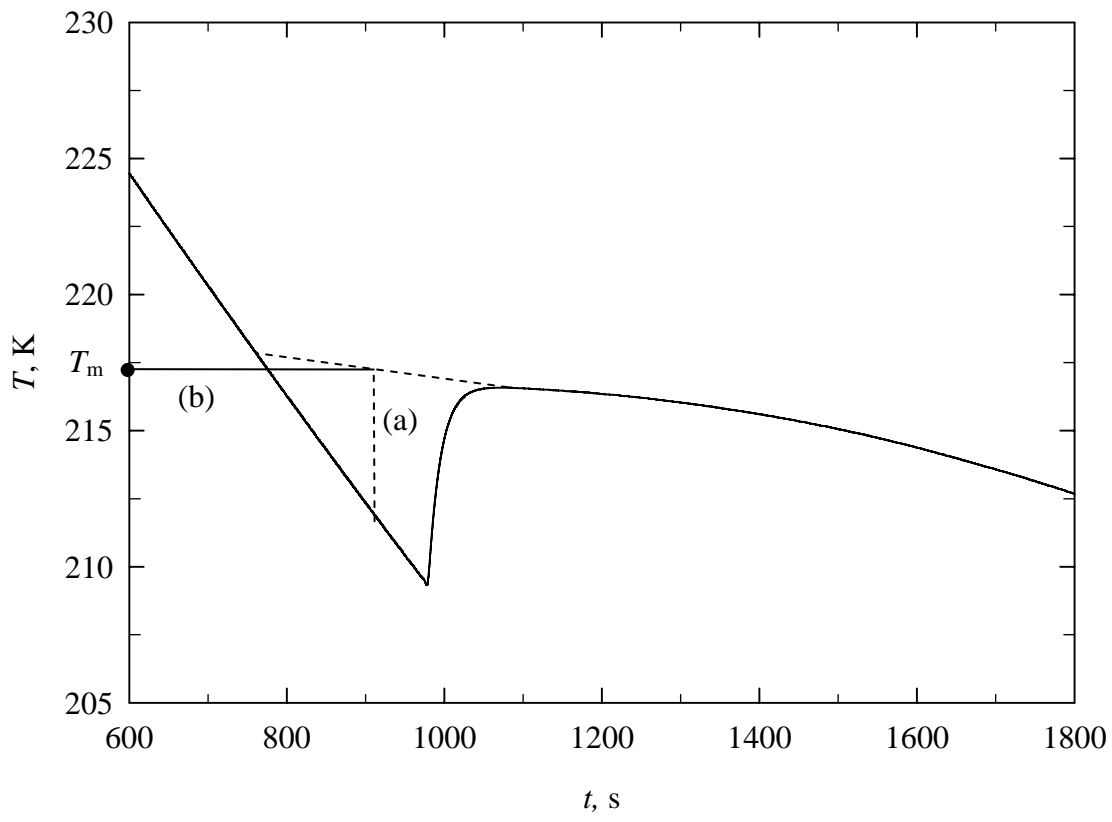


Figure 2.

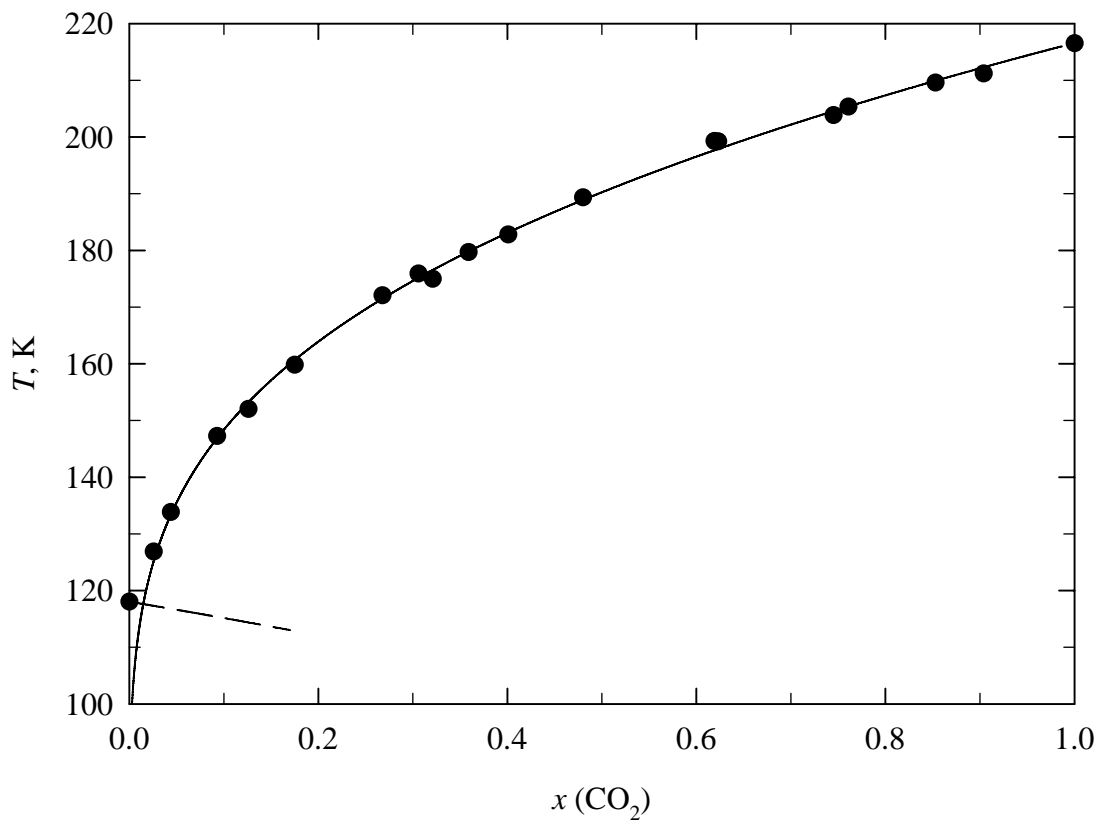


Figure 3.

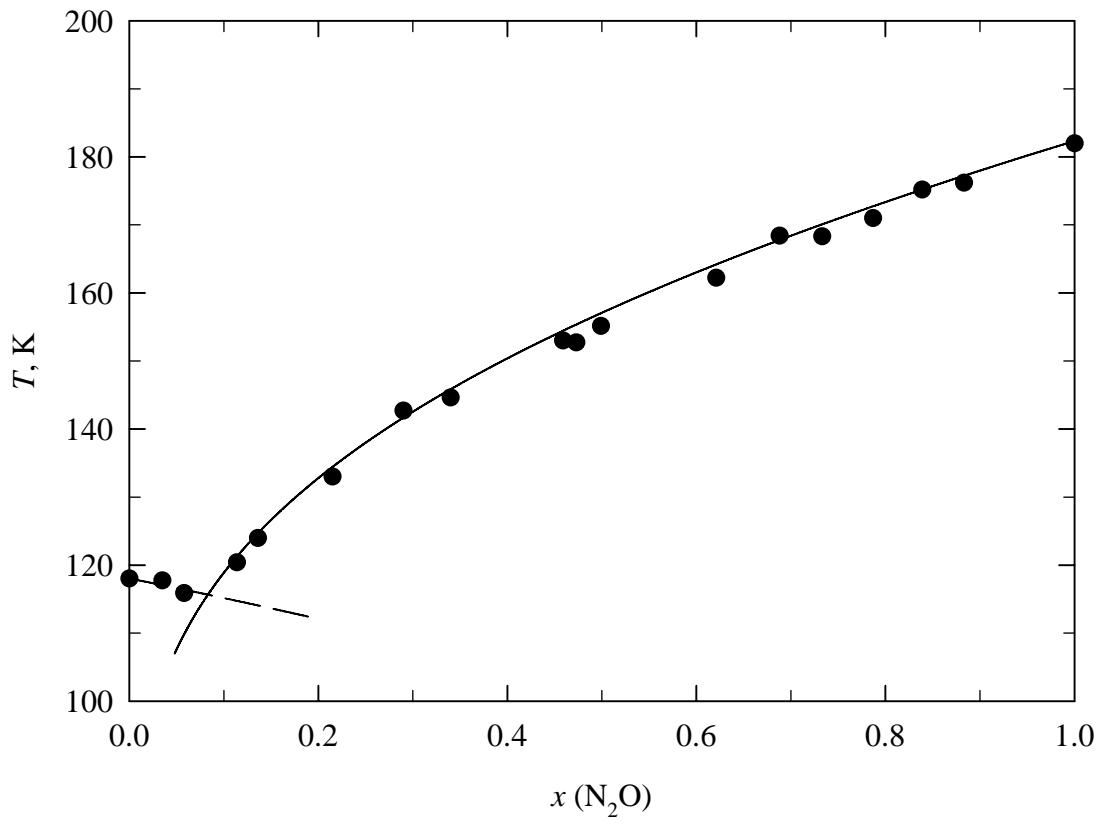


Figure 4.